

INTEGRATING MODELING AND SIMULATION TOOLS WITH LEARNINGS FROM NATURE: A METHODOLOGY FOR FORM GENERATION BY EMULATING THE CONSTRUCTAL LAW OF NATURE

Mehdi Azizkhani, Juan-Carlos Baltazar
Texas A&M University, College Station, TX

ABSTRACT

The purpose of this paper is to illustrate a methodology for integrating the learnings from nature with modeling and simulation tools for form configuration of building components in the early phases of design. Although the form configurations of living organisms may look random at first sight, the “constructal law” of nature governs these configurations for a continuously optimized performance such as in the case of the branching patterns of a tree. In this performance, the goal is to minimize the flow resistance subject to global fitness constraints of time, space, and weight. In this paper, first the principles of the constructal law have been qualitatively and quantitatively discussed. Second, following these principles and using Rhino/Grasshopper and the genetic algorithm, the form of a test case office plan as well as the configuration of its supply duct system have been optimized. Using Autodesk CFD, the air flow within the proposed duct system has been simulated, which shows a considerably better performance compared with the typical plenum duct system.

INTRODUCTION

Within the last decade, design disciplines have experienced a leap in the application of biomimicry as an approach for good abstraction of nature’s genius. By looking at living organisms in nature, designers can emulate the laws that govern their evolutionary optimization and successful adaptation. A case in point is the tree structure network in nature which has been evolved through its constructs over 3.8 billion years (Benyus, 1999; Azizkhani, 2015). River basins, blood vessels, and plants leaves represent a few examples of these constructs. Branching tree networks and their configurations have been studied extensively which show their performance in many cases can exceed manmade structures because of a lower flow resistance through their optimized conduit forms (Kou et al.,

2014). For example, Cecil Murray studied the blood vessel system as early as the 1920s (Murray, 1926; Sherman, 1981). Murray’s Law shows that there is an optimum relationship between the diameters of the human body vessels to carry the blood within an appropriate time and through the minimum work and flow resistance. This relationship between the diameters of the parent vessel (D_k) and the two daughter branches (D_{k+1}) as explained by Xu et al. (2009) can be expressed in the form of equation (1):

$$D_{k+1}/D_k = 2^{-1/3} \quad (1)$$

The application of this relationship for water transportation in plants has also been verified through experimentation (McCulloh et al., 2003). Similar studies and researches have been conducted on the functional organizations of the mammals’ lung systems and termite mounds’ air conduits (Liu et al., 2003; Soar and Tuner, 2008). More recently, Bejan and Lorente (2008) have addressed the tree network configurations in nature and the reasons behind their optimized structure. For a finite-size system to persist in time, it must evolve such that it provides easier access (i.e., minimum flow resistance with respect to global constraints of time, weight, and space) to the imposed currents that flow through it. The resulting structure has been named “constructal design” and the law from which the design develops is “constructal law” (Bejan and Lorente, 2008).

Kou et al. drawing on Bejan’s studies have explored the optimum design of the whole structure of the tree network systems and the effects of various structural parameters under different types of flow. For the laminar flow and turbulent flow resistance in smooth pipes of a tree network, they have derived equations (2) and (3) respectively (Kou et al., 2014):

$$R^+ = \left[\frac{1-\gamma^{m+1}}{1-\gamma} \right]^3 \left(\frac{1-N\beta^2\gamma}{1-(N\beta^2\gamma)^{m+1}} \right)^2 \left[\frac{1-\frac{\gamma}{NB^4}}{1-\left(\frac{\gamma}{N\beta^4}\right)^{m+1}} \right] \quad (2)$$

$$R^+ = \left[\frac{1-\gamma^{m+1}}{1-\gamma} \right]^{17/5} \left(\frac{1-N\beta^2\gamma}{1-(N\beta^2\gamma)^{m+1}} \right)^{12/5} \left[\frac{1-\gamma/N^{9/5}B^{24/5}}{1-(\gamma/N^{9/5}B^{24/5})^{m+1}} \right] \quad (3)$$

Although the rules governing tree network structures and their configurations have been studied in fields such as biology and engineering, they have been rarely applied in architectural design for form configuration.

MODELING AND SIMULATION

Modeling and optimization of the plan layout

Among the existing research findings on the tree-shaped structures, Bejan's and Lorente's studies seem more applicable for architectural form generation. Through quantitative analyses of the relationships between the freedom of tree forms and their flow resistance, Bejan discusses three factors influential in the performance of the tree structures which includes length of their branches, angle between their branches, and the level of pairing/branching (i.e. level zero of branching beginning from the center of the tree, level two in the next branching level, and so forth). For the length of the tree-shaped conduits, there is not a fixed law similar to Murray's law to determine the length of the branching ratio. In this case, the optimal length ratio can be determined based on constraints other than the flow resistance such as the area and volume (Xu et al., 2009). However, in the case of one level of T-shaped single branching, Bejan defines the optimal length branching ratio as same as the diameter branching ratio via minimizing the flow resistance under fixed volume and area constraints (2008).

While Bejan and Lorente propose an angle of 75 degrees between symmetrical branches for an optimized performance, this angle should be modified at each level to make sure that the last level of branches will not go beyond the existing boundary of the tree structure. When the distance between nodes on the perimeter of the tree structure is smaller than, but comparable with, the radius of the tree structure, the best form as shown in Figure 1 has only one level of branching with three inner nodes.

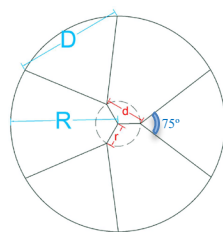


Figure 1 The best tree form for the outside circle when D is smaller than, but comparable with R , and for the inner circle when d is larger than r

However, when the distance between each two sequential nodes is larger than the structure's radius the best form develops from connecting the central point to three equidistant points around it. In this case, the angle between two neighboring branches will be 120 degrees. (Bejan and Lorente, 2008, p.127)

Following these principles for the optimization of the tree networks, the minimum flow resistance tree architecture with one level of branching was used to define the network of air distribution in a hypothetical, small office building as a test case. The selection of the tree network was based on the size of the existing office building to correspond in size and dimensions, and is expandable according to Bejan's chart on the relationship between form of tree structures and their flow resistance (Bejan and Lorente, 2008, p.135).

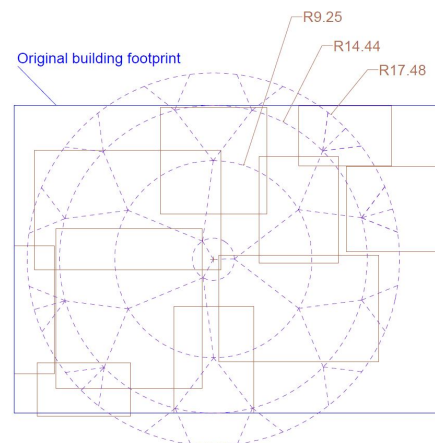
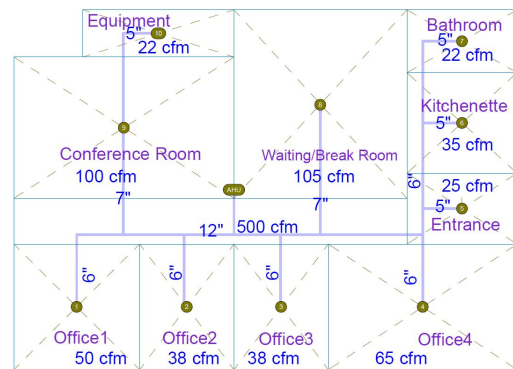


Figure 2 The office plan used as a test case in existing condition (top) and after aligning its rooms centers with the tree structure nodes (bottom)

The layout of the existing office building was changed by extracting each individual room of the office plan in its original form and size to align its center with the appropriate node of the proposed tree network as shown in Figure 2. This reconfiguration process considers six

rules to reach a conceptual plan layout in the early phases of design:

- Rooms of larger size should be assigned to the nodes of the first branching level due to their need for a higher level of air volume flow rate. In a hierarchical manner other rooms will be assigned to the sequential branching levels.
- The rooms locations in the proposed plan should preserve the rule of adjacency by minimizing the distance between neighboring rooms of the original plan.
- Efforts should aim at preserving both the symmetrical form and circular perimeter of the tree network. However, to minimize the expansion of the final proposed building form beyond the existing building footprint, the tree branches may spread in length over the circular boundary and within the building's existing footprint.
- Similarly, the bifurcation angles between tree branches should be kept at 75 degrees, or an angle close to 75 degrees if constrained by the area and perimeter of the building footprint.
- The required total air volume flow rate determines the diameter of the first duct branches, and Murray's Law ratio can determine the diameters of the other branches in sequence.
- In the new plan layout, portion of the room areas which go beyond the boundary of the building footprint can be removed and used to fill the gaps in the plan. Similarly, the overlap areas between the rooms can be merged together or be removed to fill the existing gaps of the building footprint.

Since the air diffusers were at the center of each room in the original office building, the center of each room in the proposed room layout was also assigned to the location of the new diffusers. The tree structure's nodes would represent these centers. In both office plans, before and after reconfiguration of the plan layout, the main duct from the air handler unit (AHU) comes from the middle of the plan to connect to other duct branches. This location for the AHU can reduce the required duct length as well as the static pressure drop.

An optimization graph was defined in Grasshopper through the Galapagos component with its genetic algorithm to find an appropriate orientation for each room inside the original building footprint. Two principles/constraints were considered in determining the orientation of the rooms: minimizing the overlap

areas and intersections between all rooms to maintain their original sizes/dimensions as much as possible, and minimizing the number of times that each room's probable orientations would cause its sides to infringe the perimeter of the hypothetical building footprint. These principles were incorporated to the Grasshopper graph by defining penalties for each time that the generated genes do not satisfy the defined constraints. Figure 3 shows one result out of the five generated optimized genes/plans in this process for the proposed room layout and the two resulting conceptual plans in parallel with the proposed tree duct structure shown in Figure 2. In this early design configuration, using a duct chart (Grondzick and Kwok, 2014) a round duct with a diameter of 9" was selected at level zero of the branching level to correspond to the required maximum volume flow rate. This diameter reduces to 8", 7", and 6" in the sequentially connected branches based on Murray's Law ratio and the required air volume flow rate for each room.

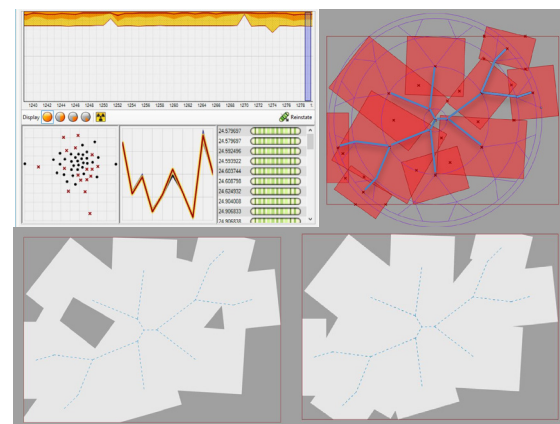


Figure 3 One of the five optimized genes using Grasshopper/Galapagos components along with the superimposed conceptual tree duct system in blue color (top) and two examples of possible conceptual plans developed from reconfiguration rules for this gene (bottom)

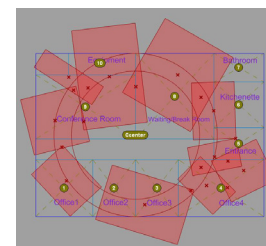


Figure 4 A conceptually optimized plan using the second approach

In another approach the form of the plan and its room layout was optimized using Grasshopper and Galapagos

plug-ins by minimizing the distance of each room's center point from the nodes of the tree structure. In this case, the radius of each of the two concentric circles was subtracted from the distances of the rooms centers from circles centers, and their absolute differences were added together through mass addition, which was set to be minimized. These differences for the larger rooms were measured from the smaller circle's center and for the smaller rooms were measured from the larger circle's center to follow the rule of assigning larger rooms to the nodes of the first branching level of the tree for receiving a higher volume flow rate. Figure 4 shows the resulting conceptual plan which does not pair with any symmetrical tree shape, and therefore, was set aside based on the third rule of the above-mentioned configuration rules.

Experimentation and CFD simulation

Autodesk CFD 2018 was used for analyzing the pressure drop of air movement inside the ducts to compare and examine the efficiency of using the proposed duct system with smooth turns versus the typical plenum duct systems with right-angle turns. The duct branches were modeled in Rhino to be exported to Autodesk CFD. Figure 5 shows the final modeled tree duct form based on the explained modeling process with two different duct profiles versus the existing office building's duct form.

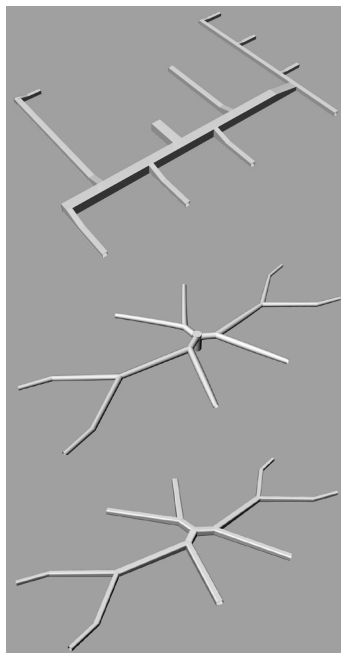


Figure 5 The concept of existing office building's duct system followed by the proposed tree duct structure with two different profiles modeled in Rhino for the optimized plan layout

For the purpose of comparison, one branch of the proposed tree duct structure and one branch from the usual duct system were selected. This selection is based on four criteria/reasons. First, the selected duct branch should connect the same points of A (air entrance) and B (air discharge) in both of the duct systems as shown in Figure 6. The distance between these two points is the maximum existing length between an air diffuser and the main air entrance from the air handler unit at the center of the plan. Therefore, point B should have a higher pressure drop. Second, the three duct turns between points A and B provide a better sample for analyzing the flow pressure drop and turbulence at each turn. Third, focusing the analysis on one branch rather than the whole duct system can reduce the number of confounding variables as well as the considerable time usually required for CFD simulations.

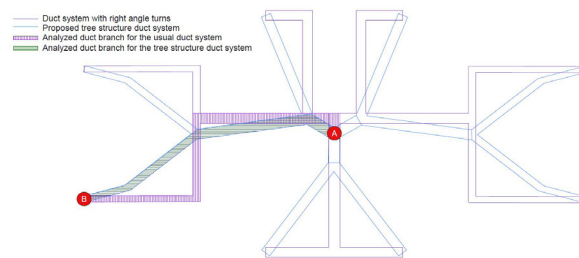


Figure 6 The duct branches between point A and B selected for CFD analysis which are extracted from the two duct systems (usual system and tree system) corresponding to the proposed plan layout

Lastly, the air flow should have an entrance long enough to be fully developed in velocity before reaching any section of the duct chosen for profile analysis (Fox et al., 2015; Autodesk CFD, 2018). Because of the required entrance length for the flow, it is more reliable to focus on the simulation of air flow at the farthest point (point B) in which the flow reaches the minimum diameter of air outlet with 6" and 22 cfm flow rate. The following paragraph will better clarify the reason for the selection of point B in relation to the effect of entrance length on simulation results.

The entrance length can be expressed with the dimensionless Entrance length number (El) as

$$El = l_e / d \quad (4)$$

Based on equation (5) the Reynolds number (Re) for air inside the duct equals 3.86×10^4 which shows the air flow is turbulent.

$$Re = \frac{\rho V D}{\mu} \quad (5)$$

The assumptions of the condition for equation (5) include free-stream fluid velocity (V) of 500ft/min

(2.54 m/s), duct diameter (D) of 9" (0.23m), and dynamic fluid viscosity (μ) of 1.817×10^{-4} poise (1.817×10^{-5} Pa-s). The Entrance length number correlation with the Reynolds number for turbulent flow can be expressed as:

$$El_{\text{turbulent}} = 4.4 \text{ Re}^{1/6} \quad (6)$$

Using equations (4) to (6), the entrance length to a fully developed velocity profile (le) will be about 25 times of the duct diameter. For example, for a duct with 9" diameter an entrance length of 19' and for a duct with 6" diameter, almost 12' 6" entrance length are required for the air flow before reaching a fully developed velocity profile in simulations. Therefore, for a more reliable result the air outlet with maximum entrance length and minimum duct diameter, which is the diffuser at point B connected to a 6" duct, was selected.

In the current study the CFD simulation assumes an environmental pressure of 100 kPa at 20°C and uses the Advection 5 solution control of the Autodesk CFD, which follows the Petrov–Galerkin method (Reddy, 2006). For this simulation the SST K-Omega turbulence model was applied which is a two-equation eddy-viscosity model. As a hybrid model SST K-Omega uses the Wilcox k-omega model near the wall and the k-epsilon model in the fluid free stream (Autodesk CFD, 2018). A variable air material was assigned to the profile of the fluid component. The length of the examined duct branch between points A and B in the two duct systems is 22.6' for the straight plenum duct system and 18' for the tree structure duct system.

Table 1 Simulation features for the two duct systems

SIMULATION FEATURES	SIMULATION 1	SIMULATION 2
Duct System	Usual right angle plenum system	Proposed tree structure system
Simulated Duct Length	22.6'	18'
Mesh Size	0.25	0.2
Environmental Condition	100 kPa and 20°C	100 kPa and 20°C
CFD Model	SST K-Omega	
Advection	Advection 5/ Modified Petrov-Galerkin	
Iterations	3000	
Boundary Conditions	Outlet: Volume flow rate of 22 cfm Inlet: Gage zero static pressure	

The boundary conditions of the simulations include gage zero static pressure at the air inlet of the duct branch and 22 cfm volume flow rate at the outlet. A building of this size usually has a static pressure of

about 1 in.H₂O. However, this study focuses on conceptually comparing the pressure drop between the two cases and here the boundary condition for both duct branches is the same. The results of simulations can reveal how much additional or less pressure is required at the air inlet. Figures 7 and 8 show the results of CFD simulations and table 1 summarizes the features of the simulations for each of the two duct systems.

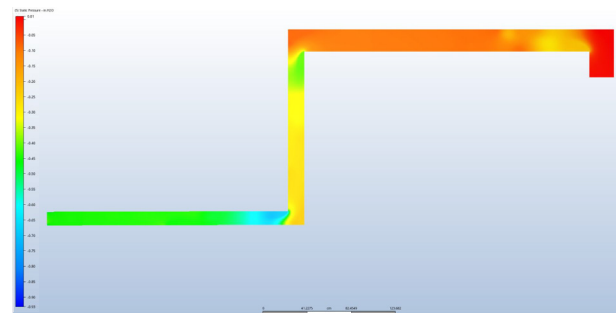


Figure 7 CFD simulation results for the duct branch between point A and B in the right angle duct system showing the static pressure drop of about 55%

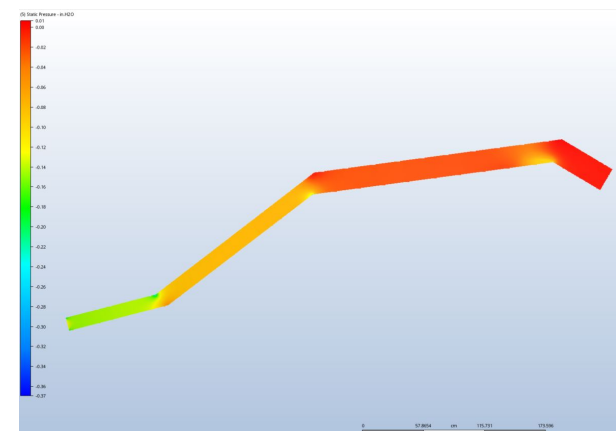


Figure 8 CFD simulation results for the duct branch between point A and B in the tree structure duct system showing the static pressure drop of about 37%

DISCUSSION AND RESULT ANALYSIS

Comparison between figures 8 and 7 clearly reveals the first advantage of using the proposed tree duct system versus the usual duct system. The former has a static pressure drop of 34% to 37% as it approaches the air outlet at point B, while this number for the right angle duct system shows about 55% pressure drop. Having

smoother turn angles, optimized ratio between duct diameters based on Murray's Law, and shorter duct lengths have provided an overall better performance in the tree-structure duct system versus the typical plenum system. The static pressure drop could be lower at point B for the tree duct branch if the boundary constraint of the building footprint was removed to extend the last portion of the duct branch beyond the existing boundary. In other words, the length of the last duct branch with 6" diameter is shorter than what it should be based on Constructal Law and Murray's Law.

Resulting from non-straight angles, a lower level of turbulence at each duct turn represents the second advantage of using the tree structure in duct design. The color scheme of the static air pressure drop in figure 8 clearly shows that, compared with the usual duct systems with 90-degree corners, the air can smoothly move inside the tree duct branch with fewer obstructions on its way. Figure 7 illustrates how the static pressure in the profile of the flow near each right angle corner drops about 25% to 40% before it regains a constant pressure inside the straight portion of the duct branch. The highest pressure drop is for that portion of the branch which has the smallest duct diameter. In contrast to the duct branch with right angles, the large areas of air turbulence are not observable in the smooth turns of the tree duct structure. The visible turbulent areas at the corners of the tree structure are very small in comparison with those of the right-angle duct system. The static pressure drop at the corners of the tree structure duct is between 5% to 10%, which is about 1/5 of the pressure drop in the right-angle duct system, and requires less time for the flow to gain a constant static pressure and a uniform profile after each turn.

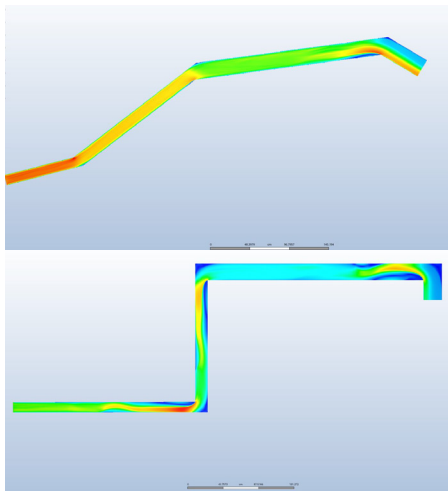


Figure 9 CFD simulation results showing the change of air velocity in one branch of each duct system

Figures 9 shows the air velocity change inside the duct branches under analysis. It is visible that the span of velocity change in each straight portion of the duct branch is considerably higher in the right angle duct system. This wider span of velocity change can evidence a higher level of turbulent flow in the right angle duct system.

CONCLUSION

This paper demonstrated a conceptual methodology of form generation in the early phases of design to define a building's plan layout and its corresponding duct system. In this methodology nature becomes a source of inspiration with its optimized tree structures which can reduce the flow resistance with respect to existing constraints of weight, time, and space. In nature, form follows flow and the flow of fluids is only one of the many examples upon which nature develops its optimized constructs. Constructal Law and Murray's Law demonstrate some principles about the conduits ratios and their bifurcation angles governing the function of these constructs for the ease of flow. These principles can be extracted and conceptualized for application in building envelope and system components to reach a better building performance.

By looking at these principles this study modeled and examined the performance of two different duct systems including the usual duct system with right-angle turns versus the tree structure duct system with smooth turns. The simulation results showed that the right angle duct systems have a higher static pressure drop compared with tree-structure ducts. The use of optimized bifurcation angles and diameter ratios between duct branches in a tree structure can considerably reduce the pressure drop and increase the overall performance of the duct system. This study limited the simulation analysis to one set of sequential branches for the two duct systems while isolating it from other branches. Therefore, analyzing the function of all the duct branches in the system in relation to each other can be a next step for reaching a better perception of the actual performance of the whole duct system.

The focus of the current experiment was on tree structures that are symmetrical in plan; however, using asymmetrical organic tree structures is another possibility for form generation in design which requires further research and experimentation. Although in this paper the form of the plan was defined based on an optimized structure for flow distribution, other design qualities such as visual, spatial, and thermal comfort should be also studied to reach a more inclusive result for the form of the plan with respect to building

performance qualities. Therefore, the generated forms as mentioned in this paper should be considered conceptual plans for further exploration through other building performance qualities and design factors.

NOMENCLATURES

D_k	Diameter of the parent vessel
D_{k+1}	Diameter of the daughter branch
D, d	Duct diameter
R^+	Flow resistance
Re	Reynolds number
m	Total number of branching levels
N	Branching number
γ	Ratio of the length
β	Ratio of the diameter of the channel
El	Entrance Length Number
le	Length to a fully developed velocity profile
ρ	Fluid density
V	Free-stream fluid velocity
μ	Dynamic fluid viscosity

REFERENCES

- Autodesk CFD. 2018. Physical Models. Retrieved January 2018 from <https://knowledge.autodesk.com/support/cfd>
- Azizkhani, M. (2015), Biomimicry Versus Machinery: the Notion of Functionality in Design, 49th International Conference of the Architectural Science Association 2015, Melbourne, Australia.
- Bejan, A., Lorente, S. 2008. Design with Constructal Theory, Wiley, Hoboken, New Jersey.
- Bejan, A. 2016. Life and Evolution as Physics, Communicative & Integrative Biology, 9:3, DOI: 10.1080/19420889.2016.1172159.
- Benyus, J. 1999. Biomimicry: Innovation Inspired By Nature, Morrow, New York.
- Fox, R.W., McDonald, A.T., Pritchard, P. J., Mitchell, J.W. 2015. Fox and McDonald's Introduction to Fluid Mechanics. 9th edition, John Wiley & Sons, Hoboken, New Jersey.
- Grondzik, W.T. and Kwok, G. A. 2014. Mechanical and Electrical Equipment for Buildings, Wiley, Hoboken, New Jersey.
- Kou, J., Chen, Y., Zhou, X., Lu, H., Wu, F., Fan, J. 2014. Optimal Structure of Tree-Like Branching Networks for Fluid Flow, Physica A, 393, 527-534.
- Liu, Y., So, R.M.C., Zhang, C.H. 2003. Modeling the Bifurcating Flow in an Asymmetric Human Lung Airway, Journal of Biomechanics, 36, 951-959.
- McCulloh, K.A., Sperry, J.S., Adler F.R. 2003, Water Transport in Plants Obeys Murray's Law, Nature 421, 939-942.
- Murray, C. D. (1926). The Physiological Principle of Minimum Work: The Vascular System and the Cost of Blood Volume. Proceedings of the National Academy of Sciences of the United States of America. 12 (3): 207-214. Doi:10.1073/pnas.12.3.20.
- Reddy, J. N. 2006. An Introduction to the Finite Element Method, McGraw-Hill.
- Sherman, T.F. 1981. On Connecting Large Vessels to Small: The Meaning of Murray's law, Journal of Physiology, 78, 431-453.
- Soar, R.C., Tuner, J. S. 2008. Beyond Biomimicry: What Termites Can Tell Us About Realizing the Living Building, First International Conference on Industrialized Intelligent Construction (I3CON), Loughborough University, UK.
- Xu, P., Wang, X., Mujumdar, A., Yap, C., Yu, B. 2009. Thermal Characteristics of Tree-Shaped Microchannel Nets With/Without Loops. International Journal Of Thermal Sciences, 48, 2139-2147. Doi:10.1016/j.ijthermalsci.2009.03.018